

# STABLE SPIN DIRECTION MEASUREMENTS AT RHIC WITH POLARIZED PROTON BEAMS\*

V. Schoefer<sup>†</sup>, E.C.Aschenauer, H. Huang, F. Méot, V. Ptitsyn, V. H. Ranjbar  
Brookhaven National Laboratory, Upton, NY, USA

## Abstract

We describe methods for measuring the three-dimensional stable spin vector at the STAR detector (using STAR local polarimetry) and at the proton-Carbon coulomb nuclear interaction polarimeter at the 12 o'clock RHIC interaction region (hereafter the pC polarimeter). These polarimeters can only provide information about the two transverse components of the stable spin direction. If a known, local spin rotation can be generated at the location of the polarimeter, then the longitudinal component can be calculated by comparing the transverse components before and after the rotation. At STAR the stable spin direction can be rotated using the helical dipole spin rotators. At the pC polarimeter, a local horizontal orbital angle is introduced to rotate the stable spin direction. The stable spin direction at the hydrogen jet polarimeter is determined by transporting the spin vector at the pC polarimeter target to the location of the jet using a Zgoubi model.

## INTRODUCTION

For a proton launched in a synchrotron ring, we may define a stable spin direction. If the proton is launched with its spin aligned (or anti-aligned) with this direction, the proton's spin direction will repeat turn-to-turn.

In RHIC, a pair of helical dipole snakes is used to fix the stable spin direction in the vertical orientation (for an ideal, error-free accelerator) [1, 2]. However, in the presence of imperfection resonances (due to vertical quadrupole misalignment or residual orbit error, for example), the stable spin direction can be moved away from the vertical. Sources of the spin tilt at RHIC store energy have been studied previously [3, 4]. These deviations from an ideal lattice make it necessary to measure the stable spin direction in order to properly calibrate polarization measurements and determine their impact on the physics process at the point of collision.

Additionally, in Run 22, two coils in one of the snakes in the Blue ring failed and in order to continue operation, the remaining two modules in that snake were reconfigured as a partial snake (one that rotates the spin vector by an angle less than 180°). This configuration breaks the symmetry of the two-full-snake configuration which results in an additional contribution to the spin tilt, since the partial snake no longer guarantees energy independent vertical stable spin direction. The Yellow ring was unaffected and still had two nominally full snakes.

\* Work supported by Brookhaven Science Associates, LLC under Contract No. DE-SC0012704 with the U.S. Department of Energy.

<sup>†</sup> schoefer@bnl.gov

It should be noted also that the store energy for Run 22 was lowered for both beams from Lorentz factor  $\gamma = 271.635$  to  $\gamma = 270.938$  relative to previous RHIC runs. This change was to rotate the non-vertical stable spin direction as much as possible into the transverse plane at STAR and the pC polarimeters. All measurements described here were made during Run 22 at  $\gamma = 270.938$ . Details of this partial snake setup during Run 22 can be found in Refs. [5, 6].

## SPIN DIRECTION AT STAR

The STAR local polarimetry reports information about the transverse components of the stable spin direction as a transverse asymmetry ( $A_n$ ) and an angle,  $\theta$  of that asymmetry axis relative to the vertical axis. The stable spin direction lies along this asymmetry axis. The coordinate system is shown in Fig. 1. The coordinate axes  $\vec{x}, \vec{y}, \vec{z}$  form a right-handed coordinate system and point radially outward, vertically upward and longitudinally in the Blue beam direction respectively. The same coordinate system is used for both Blue and Yellow beams, which means the Yellow beam travels in the negative  $\vec{z}$  direction. We call the stable spin direction vector at the interaction point  $\vec{S}$  which is normalized to have magnitude one. The vector  $\vec{\rho}$  is the projection of  $\vec{S}$  onto the transverse ( $\vec{x}-\vec{y}$ ) plane with an amplitude  $\rho$  and an angle  $\theta$  with respect to the vertical axis.

The components of  $\vec{S}$  and  $\vec{\rho}$  and the measured asymmetry,  $A_N$ , are therefore related by

$$\begin{aligned} S_x &= \rho \sin \theta \\ S_y &= \rho \cos \theta \\ \rho &= \sqrt{S_x^2 + S_y^2} = \sqrt{1 - S_z^2} \\ \rho &= \frac{A_N}{A_{max}} \end{aligned} \quad (1)$$

The total asymmetry  $A_{max}$  is not directly measurable. It is the asymmetry that would be measured by transverse scattering if the stable spin direction were entirely in the transverse plane.

Inferring  $A_{max}$ , or equivalently  $S_z$ , requires measuring the purely transverse quantities  $A_n$  and  $\theta$  in at least two different orientations. A large local rotation of the stable spin direction at the STAR interaction point is possible with the helical dipole spin rotators on either side of the interaction region (IR). A schematic of the STAR IR with its spin rotators is shown in Fig. 2. A design particle exiting the RHIC arc will see spin rotations first from the rotator itself, which rotates the spin about an axis in the horizontal plane and then a rotation about the vertical due to the DX and D0 dipole magnets. The rotators and dipoles on the outgoing side of the IR serve

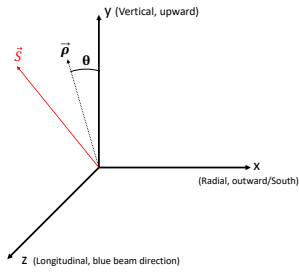


Figure 1: Coordinate system for measurements at the STAR interaction point.

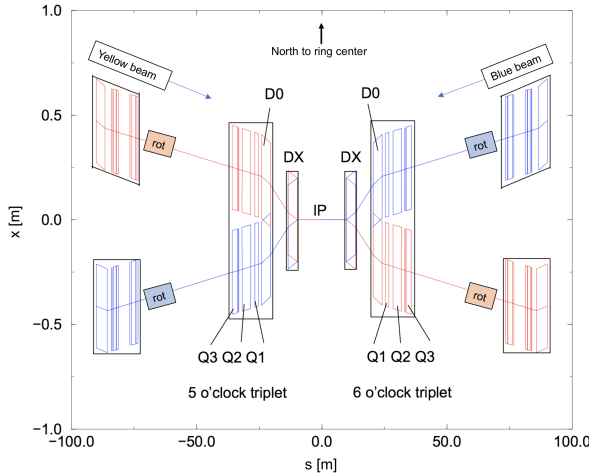


Figure 2: Schematic view of the STAR interaction region.

to return the spin direction to vertical before entry into the outgoing arc [7].

If we call the spin vector at the upstream face of the incoming rotator  $S_{arc}$ , then the initial state of the spin direction at the IP with rotators off,  $S_i$ , and the final state with rotators on,  $S_f$ , are given respectively by

$$\begin{aligned} S_i &= R_d \cdot S_{arc} \\ S_f &= R_d R_r \cdot S_{arc} \end{aligned} \quad (2)$$

where  $R_d$  and  $R_r$  are the rotation matrices representing the rotations from the DX/D0 system and the spin rotator. Subscripts  $i$  and  $f$  denote quantities at the IP before and after powering the rotators, respectively. Under the design assumption that the outgoing rotator cancels the effect of the incoming rotator  $S_{arc}$  must be the same whether the rotators are on or off. Eliminating  $S_{arc}$  and defining  $R = R_d R_r R_d^{-1}$  we have

$$S_f = R \cdot S_i \quad (3)$$

Expressing Eq. (3) explicitly in terms of the quantities defined in Eq.1 we have

$$\begin{aligned} -\rho \sin \theta_f &= -R_{11} \rho_i \sin \theta_i + R_{12} \rho_i \cos \theta_i + R_{13} S_{zi} \\ \rho \cos \theta_f &= -R_{21} \rho_i \sin \theta_i + R_{22} \rho_i \cos \theta_i + R_{23} S_{zi} \\ S_{zf} &= -R_{31} \rho_i \sin \theta_i + R_{32} \rho_i \cos \theta_i + R_{33} S_{zi} \end{aligned} \quad (4)$$

The first two lines of Eq. (4) together with the condition  $S_{zi} = \sqrt{1 - \rho_i^2}$  can be used to solve for the unknown quantities in terms of the known and measured quantities.

Defining a few convenient constants that depend only on the known matrix elements  $R_{ij}$  and the measured angles  $\theta_i, \theta_f$  we have

$$\begin{aligned} A_1 &= \frac{R_{11} \sin \theta_i - R_{12} \cos \theta_i}{\sin \theta_f} \\ A_2 &= -\frac{R_{13}}{\sin \theta_f} \\ A_3 &= \frac{-R_{21} \sin \theta_i + R_{22} \cos \theta_i}{\cos \theta_f} \\ A_4 &= \frac{R_{23}}{\cos \theta_f} \\ B &= \frac{A_3 - A_1}{A_2 - A_4} \end{aligned} \quad (5)$$

we then have

$$\begin{aligned} \rho_i &= \sqrt{\frac{1}{1 + B^2}} \\ S_{zi} &= \sqrt{\frac{B^2}{1 + B^2}} \\ S_{xi} &= \rho_i \sin \theta_i \\ S_{yi} &= \rho_i \cos \theta_i \\ A_{max} &= \frac{A_n}{\rho_o} \end{aligned} \quad (6)$$

which gives the full 3D spin vector in terms of measured quantities and known machine parameters.

The results of the measurements made during a dedicated RHIC fill are reported in Table 1. The quoted errors are statistical errors propagated from the polarimeter measurements through Eq. (6).

The values for the transport matrix  $R_{ij}$  are produced by a Zgoubi model of RHIC. Information about Zgoubi and the particular model used to generate these matrix coefficients is given in Refs. [8,9]. The Blue stable spin direction for normal physics fills has a non-vertical component that is forward (relative to the Blue beam direction) radially inward (North). The Yellow stable spin direction has a non-vertical component that is almost entirely radially outward (South), with a much smaller longitudinal component in the backward direction (relative to the Yellow beam direction).

## SPIN DIRECTION MEASUREMENTS AT THE PROTON-CARBON POLARIMETERS

The pC polarimeters are located between the Q3 and Q4 on the 1 o'clock side of RHIC IR 12. Like the STAR local

Table 1: Stable Spin Direction Measurements at the STAR Interaction Point

Ring	$\phi_o$ (deg)	$\phi_f$ (deg)	$A_o$	$A_f$	$A_{max}$	$S_x$	$S_y$	$S_z$
Blue	$-2.275 \pm 0.87$	$-178.16 \pm 1.49$	$3.588 \pm 0.046$	$0.88 \pm 0.029$	$4.370 \pm 0.053$	$-0.040 \pm 0.015$	$0.998 \pm 0.002$	$0.042 \pm 0.031$
Yellow	$8.692 \pm 0.692$	$111.596 \pm 2.326$	$3.431 \pm 0.05$	$0.653 \pm 0.023$	$3.431 \pm 0.045$	$0.151 \pm 0.011$	$0.989 \pm 0.002$	$0.003 \pm 0.006$

Table 2: Stable Spin Direction Measurements at the p-C Polarimeters in Run 22

Ring	$\psi$ (deg)	$\phi$ (deg)	$S_x$	$S_y$	$S_z$	$\chi^2$
Blue	$7.82 \pm 3.45$	$177.12 \pm 3.54$	$0.007 \pm 0.008$	$0.991 \pm 0.008$	$-0.136 \pm 0.060$	1.79
Yellow	$7.40 \pm 2.98$	$-2.56 \pm 3.64$	$-0.006 \pm 0.007$	$0.992 \pm 0.007$	$0.129 \pm 0.052$	1.14

polarimetry, the pC polarimeter can only measure the two components of the spin direction transverse to the beam direction [10]. Since this IR does not have spin rotators, the rotation of the longitudinal component of the stable spin direction into the transverse plane is accomplished instead by the introduction of a local horizontal orbit angle at the target location. For a given orbital angle change  $\Delta\theta$ , the stable spin precesses by  $G\gamma\Delta\theta$ , where  $G$  is the anomalous magnetic ratio and  $\gamma$  the Lorentz factor. The machine aperture allowed a maximum angular range of  $\pm 350\ \mu\text{rad}$ , which produced  $\pm 9^\circ$  of spin precession. At the p-Carbon location the (x,y,z)

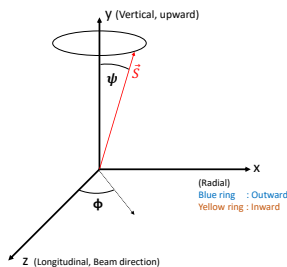


Figure 3: Coordinate system for measurements at the p-C and hydrogen jet polarimeters.

triad is (radial,vertical,longitudinal beam direction), but in the Blue ring the positive x direction is radially outward, where in the Yellow ring it is radially inward.

For a simple precession about the vertical axis, the radial component of the stable spin direction  $S_x$  has the form

$$\begin{aligned} S_x &= A \sin(\Delta\phi + \phi) \\ A &= \sin\psi \end{aligned} \quad (7)$$

The angles  $\psi$  and  $\phi$  are spherical coordinates denoting the angles with respect to the vertical and longitudinal axes, respectively (see Fig. 3,  $\Delta\phi$  is the precession angle about the vertical caused by the horizontal orbit angle change, and  $\psi$  and  $\phi$  are the unknown orientation angles of the spin vector without the additional precession and  $S_x$  is the radial component of the spin direction measured by the polarimeter. Equation 7 can be fit to measurements of  $S_x$  as a function of  $\Delta\phi$  to infer values for  $\psi$  and  $\phi$  which together fully determine the spin orientation.

The measurement results from RHIC Run 22 are shown together with the sinusoidal fits in Fig 4 and the results of the fit are summarized in Table 2.

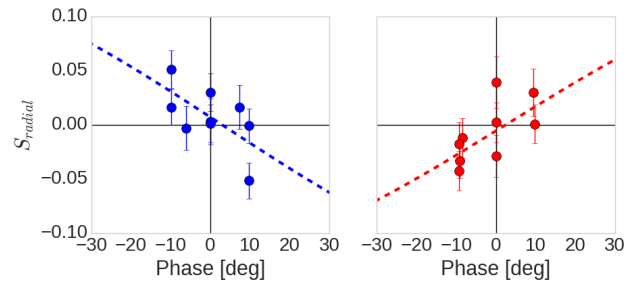


Figure 4: p-Carbon polarimeter measurements of the radial component of the stable spin direction in the Blue (left) and Yellow (right) rings as a function of the spin precession angle about the vertical induced by an applied horizontal orbital angle. Each point represents the average of several polarization measurements. The dashed line indicates the sinusoidal fit.

In both rings the deviation away from the vertical is directed mainly in the longitudinal direction (Blue tipped slightly forward, Yellow backward, relative to their respective beam directions).

The polarized hydrogen jet polarimeter (H-Jet) is located at the interaction point in the center of the common pipe at 12 o'clock in the RHIC ring. The H-Jet is the only absolute polarimeter in the RHIC rings and is used to calibrate the relative polarization measurements made with the pC polarimeters [11]. The H-Jet measures only the vertical component of the polarization with a low event rate (8 hours for a 2% statistical error), which makes extensive orientation scans impractical. Instead, the spin orientation measured at the pC polarimeter is transported to the location of the H-Jet using a matrix generated by Zgoubi. This matrix includes the effects of the horizontal dipoles between the pC and H-Jet locations as well as the vertical bumps used to separate the two beams in the common section at the H-Jet [9]. The vertical component at the H-Jet is calculated to be  $0.991 \pm 0.008$  (Blue) and  $0.992 \pm 0.006$  (Yellow), indicating only a small calibration correction factor.

## CONCLUSIONS

Methods for measuring the full 3D stable spin direction at locations in RHIC where only the transverse components of the stable spin direction were derived. Results of these measurements from RHIC Run 22 were also presented.

## REFERENCES

- [1] S. Y. Lee, *Spin Dynamics and Snakes in Synchrotrons*, World Scientific, 1997.
- [2] I. Alekseev *et al.*, “Polarized Proton collider at RHIC”, *Nucl. Instrum. Methods Phys. Res., Sect. A*, vol. 499, pp. 392–414, 2003. doi:10.1016/S0168-9002(02)01946-0
- [3] V. H. Ranjbar *et al.*, “RHIC Polarized Proton Operation for 2017”, in *Proc. IPAC’17*, Copenhagen, Denmark, May 2017, pp. 2188–2190. doi:10.18429/JACoW-IPAC2017-TUPVA050
- [4] V. H. Ranjbar, E. C. Aschenauer, H. Huang, A. Marusic, F. Mèot, and V. Schoefer, “Modeling RHIC Spin Tilt as Lattice Imperfections”, in *Proc. IPAC22*, Bangkok, Thailand, Jun. 2022, pp. 1884–1885. doi:10.18429/JACoW-IPAC2022-WEPOPT020
- [5] V. Schoefer *et al.*, “RHIC Polarized Proton Operation in Run 22”, in *Proc. IPAC22*, Bangkok, Thailand, Jun. 2022, pp. 1765–1767. doi:10.18429/JACoW-IPAC2022-WEPOST031
- [6] F. Mèot *et al.*, “RHIC Blue Snake Blues”, in *Proc. IPAC’22*, Bangkok, Thailand, Jun. 2022, pp. 1881–1883. doi:10.18429/JACoW-IPAC2022-WEPOPT019
- [7] T. Roser *et al.*, *Configuration Manual: Polarized Proton Collider at RHIC*, 2006.
- [8] F. Mèot, Zgoubi, <http://sourceforge.net/projects/zgoubi/>.
- [9] F. Mèot, V. Schoefer, Transport of  $\vec{n}_0$  “Spin Vector in STAR and Polarimetry Regions for RHIC Run 22 Optics”, Brookhaven National Lab, USA, C-AD Tech Note, C-AD/AP/663, 2022.
- [10] I. Nakagawa *et al.*, “p-Carbon Polarimetry at RHIC”, *AIP Conf. Proc.*, vol. 980, p. 380, 2008. doi:10.1063/1.2888112
- [11] A. Zelenski *et al.*, “Absolute polarized H-jet polarimeter development at RHIC”, *Nucl. Instrum. Methods Phys. Res., Sect. A*, vol. 536, p.248, 2005. doi:10.1016/j.nima.2004.08.080